ELSEVIER

Fuel Processing Technology 86 (2005) 1627–1645

FUEL PROCESSING TECHNOLOGY

www.elsevier.com/locate/fuproc

Activation of magnesium rich minerals as carbonation feedstock materials for CO_2 sequestration

M.M. Maroto-Valer[a,*,1], D.J. Fauth[b], M.E. Kuchta[a], Y. Zhang[a], J.M. Andrésen[a,1]

[a]*The Energy Institute, The Pennsylvania State University, 405 Academic Activities Bldg., University Park, PA 16802, United States*

[b]*U.S. Department of Energy, National Energy Technology Laboratory, Pittsburgh, PA 15236, United States*

Abstract

Mineral carbonation, the reaction of magnesium-rich minerals such as olivine and serpentine with CO_2 to form stable mineral carbonates, is a novel and promising approach to carbon sequestration. However, the preparation of the minerals prior to carbonation can be energy intensive, where some current studies have been exploring extensive pulverization of the minerals below 37 μm, heat treatment of minerals up to 650 °C, prior separation of CO_2 from flue gases, and carbonation at high pressures, temperatures and long reaction times of up to 125 atm, 185 °C and 6 h, respectively. Thus, the objective of the mineral activation concept is to promote and accelerate carbonation reaction rates and efficiencies through surface activation to the extent that such rigorous reaction conditions were not required. The physical activations were performed with air and steam, while chemical activations were performed with a suite of acids and bases. The parent serpentine, activated serpentines, and carbonation products were characterized to determine their surface properties and assess their potential as carbonation minerals. The results indicate that the surface area of the raw serpentine, which is approximately 8 m^2/g, can be increased through physical and chemical activation methods to over 330 m^2/g. The chemical activations were more effective than the physical activations at increasing the surface area, with the 650 °C steam activated serpentine presenting a surface area of only 17 m^2/g. Sulfuric acid was the most effective acid used during the chemical activations,

* Corresponding author. Tel.: +44 115 846 6893; fax.: +44 115 951 4115.
E-mail address: Mercedes.maroto-valer@nottingham.ac.uk (M.M. Maroto-Valer).

[1] Present address: School of Chemical, Environmental and Mining Engineering, University of Nottingham, University Park, Nottingham NG7 2RD, UK.

0378-3820/$ - see front matter
doi:10.1016/j.fuproc.2005.01.017

resulting in surface areas greater than 330 m^2/g. Several of the samples produced underwent varying degrees of carbonation. The steam activated serpentine underwent a 60% conversion to magnesite at 155 °C and 126 atm in 1 h, while the parent sample only exhibited a 7% conversion. The most promising results came from the carbonation of the extracted $Mg(OH)_2$ solution, where, based on the amount of magnesium recovered in the precipitate after the 3.5 h reaction, the carbonation efficiency was estimated to be at least 53%. Reaction products included several hydrated magnesium carbonate compounds. The carbonation reaction was conducted at ambient temperature, 20 °C, and low pressure, 45 atm.

Keywords: Carbon dioxide sequestration; Mineral activation; Mineral carbonation

1. Introduction

Fossil fuels have been the world's primary source of energy for well over a century. They currently account for nearly 85% of the world's energy supply—a trend that is expected to continue throughout the 21st century [1–5]. However, the use of fossil fuels does not come without repercussions. Perhaps the most difficult challenges that have arisen from the utilization of fossil fuels are the issues of greenhouse gas emissions and global climate change. Although passionate debates over global climate change are ongoing, the general consensus is that global warming is a reality [6–8]. This climatic variation is inevitably associated with greenhouse gas emissions–particularly carbon dioxide (CO_2)–originating from the consumption of fossil fuels. In the U.S., CO_2 emissions from fossil fuel burning account for nearly 82% of the total anthropogenic greenhouse gas emissions [9]. Overall, atmospheric concentrations of greenhouse gases have risen significantly during the last 60 years, with CO_2 concentrations rising over 30% compared to pre-industrial levels [3,4,7,10,11]. Consequently, focus has been placed on managing CO_2 emissions. Carbon management can be achieved through three different, but complimentary, approaches: increasing the efficiency of energy conversion, using low-carbon or carbon-free energy sources, and capturing and sequestering CO_2 emissions. It is generally accepted that the first two options will only provide incremental improvements. Therefore, carbon sequestration technologies must be developed to achieve zero emissions [12].

Mineral carbonation, which involves the reaction of magnesium-rich minerals with CO_2 to form geologically stable mineral carbonates, has been proposed as a promising CO_2 sequestration technology. Suitable feedstocks include olivine (Mg_2SiO_4) and serpentine ($Mg_3Si_2O_5(OH)_4$) minerals, and the general reaction is shown in Eq. (1.1).

$$(Mg, Ca)_x Si_y O_{x+2y} + xCO_2 \rightarrow x(Mg, Ca)CO_3 + ySiO_2 \quad (1.1)$$

Mineral carbonation results in the storage of CO_2 in solid form as a stable, environmentally benign mineral carbonate. In fact, the process emulates natural chemical transformations that occur spontaneously in nature—the weathering of rocks over geologic time scales [5,13,14]. The resulting carbonate product is known to be stable over geologic time frames, with mineral carbonates being the ground state of carbon. The energy state of

a mineral carbonate is 60 to 180 kJ/mol lower than CO_2, which is 400 kJ/mol lower than carbon [15]. Consequently, sequestration in the form of a carbonate ensures long-term fixation of CO_2 rather than temporary storage. Legacy issues for future generations and the need for expensive monitoring are thereby eliminated. Also avoided is the risk of any accidental release of stored CO_2 [16].

A vast natural abundance of magnesium-rich silicate minerals, especially serpentines, exists across the globe, where many of the large deposits in the U.S. lie near major population areas, such as along the Appalachian mountain chain on the East Coast and the Cordilleran mountain chain on the West Coast [17]. Previous studies have determined that several ultramafic complexes in North America contain sufficient quantities of magnesium silicate minerals to provide raw materials for the carbonation of all U.S. power plant CO_2 emissions for centuries [18,19]. For example, the volume of serpentine deposits in the mid-Appalachian region, approximately 30 km^3, could sequester the CO_2 emissions of a population center of 1 million people for 1600 years [17]. Furthermore, it has been determined that readily accessible deposits exist in quantities that far exceed the amount needed to carbonate all the CO_2 that could be emitted from even the most optimistic estimate of the world's fossil fuel reserves [13,17–19]. Both serpentine and olivine occur in sufficient magnitude to be considered viable candidates for mineral sequestration, although serpentine deposits are far more prolific.

The overall carbonation process is exothermic, and therefore has the potential to become economically viable [5,13,20–22]. The carbonation of olivine results in a release of 95 kJ/mol of heat, while the serpentine reaction releases 64 kJ/mol [6,13,20,22]. In addition, the ability to produce value-added products during the carbonation process, including energy and valuable metals, may further contribute to its cost effectiveness [5,6,20]. Beneficial uses of the reaction product solids, comprised primarily of magnesite (~65% by weight) and free silica (~25% by weight), may also be possible [23]. Potential uses include utilizing the product for mine reclamation or soil amendments. The magnesite could possibly replace conventional soil liming agents, while the hydrophilic free silica could improve soil water retention in arid environments [23,24]. Magnesite has also been used as a fire retardant and as filler material during the manufacturing of paint, paper, plastics, bricks, and ceramics [25]. At Albany Research Center (ARC), bricks have been made by binding magnesite with common wood glue [26]. These magnesite bricks are about 20% CO_2 by weight.

The mineral carbonation process does have some serious drawbacks, however. Although the process is exothermic in nature, it is inherently slow and occurs over thousands of years in nature [22]. In an attempt to increase the carbonation efficiency of the mineral feedstocks, several pretreatment methods have been studied, including particle communition, magnetic separation, heat treatment, various acid treatments, and HCl extraction [3,5,6,16,19,23,24,27–37]. In addition, current mineral carbonation studies are based on extensive communition of the raw minerals (<37 μm), high temperatures (>185 °C) and partial pressures (>125 atm), prior capture of the CO_2 from flue gases, heat treatment (600–650 °C), and long reaction times (>6 h). These are all energy intensive operations, where the CO_2/flue gas separation can impose an energy penalty of about 20% to the electricity output of a power plant [1]. O'Connor et al. estimates that the heat treatment, based on the serpentine heat capacity alone, requires around 200–250 kW h/ton

of serpentine, while the total estimated energy demand for heat treatment is roughly 293 kW h/ton for antigorite serpentine and 326 kW h/ton for lizardite serpentine, incurring at least a 20% energy penalty for a coal-fired power plant [22–24,38], and pilot scale communition tests to grind serpentine minerals to minus 75 μm have reported an energy penalty of 11 kW h/ton of mineral processed [39]. Further, previous studies have shown that mineral dissolution rates are surface controlled, and the carbonation reaction stops when the magnesium at the mineral's surface becomes depleted and/or blocked by mass transfer resistance [23,24]. Thus, fast reaction routes under milder regimes in a continuous integrated process as investigated here must be developed before mineral carbonation can become a cost-effective sequestration technology [40–44].

Accordingly, the focus of this work was to study mineral activation of serpentine as a route to accelerate the carbonation reaction efficiency and rate, thus eliminate the need for extensive mineral communition and heat treatment, while lowering the temperature and pressure conditions of the reaction. The parent serpentine, activated serpentines, and carbonation products were characterized by several analytical techniques to determine their surface properties and assess their potential as carbonation minerals. Physical activation was found to be a more effective technique for reducing the inherent moisture content of the serpentine, while chemical activations were more effective at increasing the surface area. It was found that the surface area of the raw serpentine, which is about 8 m^2/g, can be increased by chemical activation to nearly 330 m^2/g. Furthermore, it was determined that over 70% of the magnesium within the serpentine could be extracted through chemical activation. The carbonation reaction results varied, with several of the activated serpentines and solutions reacting with CO_2 to form magnesite and/or several types of hydrated carbonate. The steam activated serpentine underwent a 60% conversion to magnesite at 155 °C and 126 atm after 1 h. Under the same operating conditions, the parent sample only underwent a 7% conversion. The most promising results were obtained during the carbonation of an extracted $Mg(OH)_2$ solution. An estimated conversion percentage of 53% was achieved after only 3.5 h at ambient temperature (20 °C) and low CO_2 pressure (45 atm). This is indeed a significant improvement over previous studies that have required much higher temperatures (>185 °C) and pressures (>125 atm).

2. Experimental

The feedstock used for the mineral carbonation studies was a magnesium silicate hydroxide known as serpentine ($Mg_3Si_2O_5(OH)_4$) obtained from Cedar Hills Quarry in southeast Pennsylvania. Antigorite was the primary phase present in the sample, with a secondary phase existing in the form of forsterite, and 38.7 wt.% of the serpentine was MgO. Prior to the activation experiments, the mineral's reactive surface area was increased by grinding the Cedar Hills serpentine to minus 75 μm (<200 mesh). Furthermore, the sample underwent magnetic separation to remove a portion of the iron present within the serpentine, eliminating the need for a non-oxidizing environment during heat treatment. The Cedar Hills serpentine was activated through both chemical and physical means in solid or aqueous form. The solid and aqueous carbonation samples were labeled as SCS

Table 1
Nomenclature system

Sample	Solid carbonation samples	Solid carbonation products
Solids	Label	Label
Untreated parent	SCS-1	SCP-1
Air activated	SCS-2	–[a]
300 °C Steam activated	SCS-3	–[a]
650 °C Steam activated	SCS-4	SCP-4
HCl activated	SCS-5	SCP-5
H_2SO_4 activated	SCS-6	SCP-6
H_3PO_4 activated	SCS-7	SCP-7
NaOH activated	SCS-8	SCP-8
Aqueous solutions	Aqueous carbonation samples	Aqueous carbonation products
$MgSO_4$ solution	ACS-1	ACP-1
$Mg(Ac)_2$ solution[b]	ACS-2	ACP-2
$Mg(OH)_2$ solid[c]	ACS-3	ACP-3a[d], ACP-3b[d]

[a] Samples were not subjected to carbonation.
[b] Nomenclature used to represent magnesium acetate.
[c] Sample was dissolved in water prior to carbonation.
[d] ACP-3a is the first precipitate formed, ACP-3b is the second precipitate formed.

and ACS, respectively, while their corresponding carbonation products were labeled as SCP and ACP (Table 1).

The physical activations utilized steam and air to dehydroxylate and activate the samples. For the steam treatments approximately 10 g of serpentine were placed into a horizontal tube furnace under 300 mL/min of N_2. The sample was heated to the desired temperature (300 °C or 650 °C). Once this temperature was reached, water was supplied by a HPLC pump at 0.5 mL/min and carried by N_2 at 300 mL/min. The air activation was performed in a muffle furnace at 630 °C for 3 h in an open system. Other similar physical activation procedures have been reported in the literature [44,45].

The chemical activations were performed by subjecting the serpentine samples to a suite of acids and bases. Activation conditions varied by sample, with reactions conducted at ambient temperature for 24 h, at 50 °C for 8 h, and at 90 °C for 4 h. Approximately 50 g of serpentine were placed into a 2 L reaction vessel and 200 mL of distilled water was added. A magnetic stir bar was used to ensure adequate mixing throughout the activation. A hot-bath was utilized to maintain the desired reaction temperature before adding 200 mL of the selected chemical activation agent. After the desired reaction time the mixture was cooled and filtered to separate the remaining serpentine from the solution. A portion of the filtrate was recovered for further analysis. The activated serpentine was then washed with distilled water until it reached a neutral pH and the solids were dried in an oven at 110 °C for approximately 24 h. Table 2 summarizes the various chemical activations that were performed. Other chemical treatments of serpentine have also been reported in the literature [46–48].

Table 3 provides a summary of each carbonation test, including reaction temperature, pressure, time, and buffer composition. The high temperature and pressure carbonation reactions were carried out in a 1 L Hastelloy C-2000 continuous-stirred-tank-reactor

Table 2
The time and temperature, the reagents used, and the goal of each chemical activation process

Time and temperature	Reagent and sample label	Activation goal
24 h 25 °C	HCl (SCS-5)	To produce a serpentine with a high surface area and a higher reactivity towards carbonation
	H_2SO_4 (SCS-6)	
	H_3PO_4 (SCS-7)	
4 h 90 °C	NaOH (SCS-8)	
8 h 50 °C	H_2SO_4 (ACS-1)	To produce a Mg-rich $MgSO_4$ solution
	CH_3COOH (ACS-2)	To produce a Mg-rich $Mg(Ac)_2$ solution
	H_2SO_4 (ACS-3)	To produce solid $Mg(OH)_2$

(CSTR) unit. Typically, 30 g of the pulverized magnesium silicate particles were charged into the CSTR. Further, a 360 g of buffer solution was charged into the reactor, with a composition of 0.6 M $NaHCO_3$; 1.0 M NaCl. The CSTR was then sealed and purged with gaseous CO_2 and a calculated amount of liquid CO_2 was injected through the side port of the CSTR, making the final pressure 126 atm. The stirrer was set to 1000 rpm and the unit was heated to 155 °C and the reaction was allowed to continue for 1 h. The remaining CO_2 was vented and the hot carbonated slurry was flushed from the CSTR and filtered to separate solids from the aqueous buffer solution. The solids were washed until a neutral pH was obtained, and dried in air overnight at 105 °C. The low temperature and pressure carbonation reactions were performed in a 500 mL Hastelloy C-276 CSTR vessel with a similar procedure, but under much milder conditions (Table 3).

The parent serpentine, as well as the activated samples and carbonation products, were characterized by several different analytical techniques. The thermal gravimetric analysis (TGA) was performed with a Perkin Elmer TGA 7. The studies were conducted in a non-oxidizing atmosphere of nitrogen (N_2) at atmospheric pressure. Analyses were conducted over a temperature range of 25 °C to 900 °C, with a constant heating rate of 10 °C/min. The surface area, pore volume, and average pore diameter of the samples were characterized using a Quantachrome Autosorb-1 Model ASIT adsorption apparatus. Adsorption isotherms were obtained under N_2 at a temperature of 77 K. The BET surface areas were calculated using the adsorption points at the relative pressures (P/P_0) 0.05–0.25, and the total pore volume was calculated from the amount of vapor adsorbed at the relative pressure of 0.95. Taking into account the surface area and pore volume, the

Table 3
Summary of the carbonation tests, including reaction temperature, pressure, time, and buffer composition

Sample	Reaction temperature (°C)	CO_2 pressure (atm)	Reaction time (h)	Buffer composition
SCS-1, SCS-4, SCS-5, SCS-6, SCS-7, SCS-8	155	126[a]	1	0.6 M $NaHCO_3$; 1.0 M NaCl
ACS-1	20	36[b]/22[c]	6	8.11 g NaOH
ACS-2	20	45[b]/36[c]	4	1.34 g NaOH
ACS-3	20	45[b]/25[c]	3.5	Reverse osmosis water

[a] Pressure was maintained throughout the reaction.
[b] Initial pressure.
[c] Pressure recorded at the end of the reaction.

average pore diameter was then calculated by assuming that the pores were cylindrical in shape. The chemical compositions of the samples were obtained through ICP-AES analyses using a Leeman Labs PS3000UV inductively coupled plasma spectrophotometer. Both solutions and solid samples were analyzed, with the solid samples being dissolved by a lithium metaborate fusion technique before analysis. The solutions were examined for the following elements: Al, Ba, Ca, Fe, K, Mg, Mn, Na, Si, and Sr. Solid samples were analyzed for the following metal oxides: Al_2O_3, BaO, CaO, Fe_2O_3, K_2O, MgO, MnO, Na_2O, P_2O_5, SiO_2, SrO, and TiO_2. The loss on ignition (LOI) values were calculated by measuring the weight loss of the samples upon heating to 750 °C in a muffle furnace for approximately 12 h, followed by cooling in a dessicator. The mineral phases present in each sample were determined by XRD analyses. A Scintag Pad V unit with a vertical theta/2-theta goniometer was used. The unit utilized a Cu-Kα X-ray source and was operated at a voltage of 35 kV and a current of 30 mA. The samples were analyzed over a 2-theta range of 5.0° to 90.0°, with a step-scan rate of 0.1°/min. Peaks were identified using the ICDD Powder Diffraction Files. A quartz zero background holder was used to mount the powder samples during XRD analyses. A HITACHI S-3500N was used to conduct the SEM analyses. Experiments were performed using secondary electrons under high vacuum and an accelerating voltage of 20 kV. Images were taken at magnification levels up to 10,000 times, with a working distance of 7–9 mm. The powder samples were mounted on a holder using carbon tape. In addition, the samples were spattered with a thin layer of gold to provide an electrically conductive surface.

3. Results and discussion

Fig. 1 shows the TGA profiles of the physically activated samples, while Fig. 2 shows the profiles of the chemically activated samples. The weight loss of the parent sample (SCS-1) occurred in three stages where the first weight loss (25–150 °C) corresponds to adsorbed water, the second (300–375 °C) corresponds to the evolution of water of crystallization, and the final loss (>500 °C) is the evolution of hydroxyl groups. Both physically and chemically activation produced samples with significant changed TGA profiles (Figs. 1 and 2). In the case of the physically activated samples the principal weight loss shifted to higher temperatures (>600 °C), indicating that the moisture remaining after physical activation consists primarily of chemically bonded hydroxyl groups. The air (SCS-2) and high temperature steam treatments (SCS-4) were effective in removing a large fraction of these hydroxyl groups, as shown by the small degree of weight loss during TGA analyses. However, the low temperature steam treatment (SCS-3) removed mainly the adsorbed water. It did not have an impact on the strongly bonded hydroxyl groups. Thus, steam treatment at 300 °C does not appear to be an effective pretreatment option. For this reason, the serpentine activated with low temperature steam (SCS-2) was not subjected to any further analyses. The chemical activations were also relatively unsuccessful at removing the water from the parent sample (Fig. 2). Similar to the low temperature steam activation, they were only able to remove adsorbed moisture.

Table 4 lists the BET surface area, total pore volume, and average pore diameter for the untreated parent sample and the physical and chemical activated serpentine samples. The

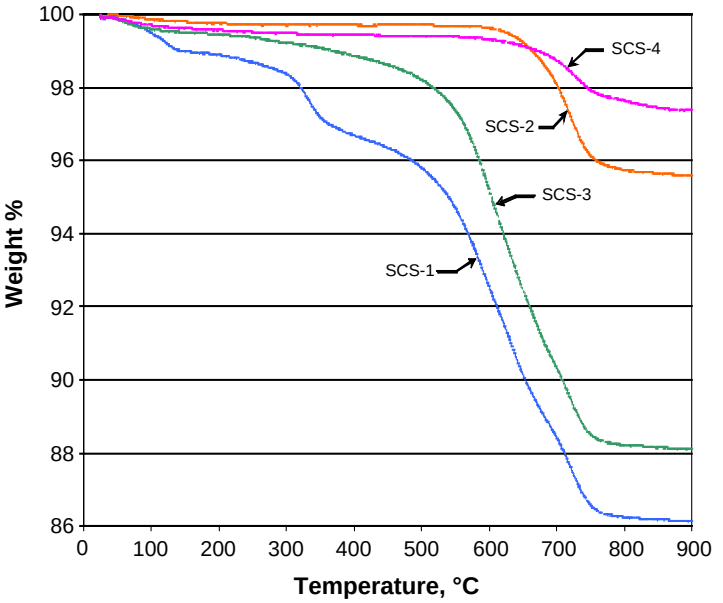

Fig. 1. Comparison of the TGA profiles of the parent serpentine and its physically activated samples.

BET surface areas indicate that several of the chemical activations were quite successful at raising the surface area of the serpentine. In fact, treatment with H_2SO_4 and H_3PO_4 increased the surface area by two orders of magnitude from 8 m^2/g for the parent

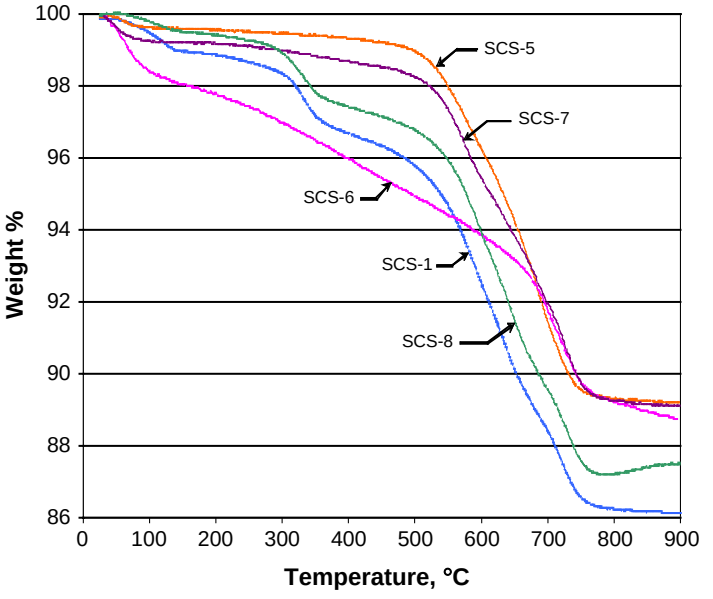

Fig. 2. Comparison of the TGA profiles of the parent serpentine and its chemically activated samples.

Table 4
BET surface area, total pore volume, and average pore diameter of the parent (SCS-1) and the physically (SCS-2, SCS-4) and chemically activated (SCS-5, SCS-6, SCS-7 and SCS-8) serpentine samples

Sample	BET surface area (m^2/g)	Total pore volume (mL/g)	Average pore diameter (nm)
SCS-1	8.2	0.017	8.5
SCS-2	17.3	0.034	7.9
SCS-4	15.8	0.035	8.8
SCS-5	79.5	0.085	4.3
SCS-6	330	0.234	2.8
SCS-7	122	0.097	3.2
SCS-8	8.7	0.023	6.1

serpentine (SCS-1) to 330 m^2/g and 122 m^2/g for SCS-6 and SCS-7, respectively. In contrast, the physical activations (SCS-2 and SCS-4) did not have a significant impact on the surface area of the mineral (17.3 m^2/g and 15.8 m^2/g, respectively), and the treatment with NaOH (SCS-8) had virtually no effect on the surface area (8.7 m^2/g). Similar to the surface area, the serpentine's total pore volume was also increased during the activations. A maximum pore volume of 0.234 mL/g was exhibited by the H_2SO_4 activated serpentine (SCS-6), compared to only 0.017 mL/g for the untreated parent sample (SCS-1). The average pore diameters were decreased, however, especially during the chemical activations. As the surface area increased, the pore diameters decreased, from 8.5 nm for the untreated parent sample (SCS-1) to as low as 2.8 nm for the H_2SO_4 activated sample (SCS-6).

Table 5 shows the LOI and ICP-AES results from the analysis of the parent (SCS-1), physically activated (SCS-4), and chemically activated (SCS-5, SCS-6, SCS-7, SCS-8) serpentine and the precipitated $Mg(OH)_2$ (ACS-3) samples. The Cedar Hills serpentine (SCS-1) was determined to be approximately 38.7% MgO by weight, with the remainder of the mineral being comprised primarily of SiO_2 (39.5%), Fe_2O_3 (4.86%), and additional

Table 5
The LOI and ICP-AES results from the analysis of the parent (SCS-1), physically activated (SCS-4), and chemically activated (SCS-5, SCS-6, SCS-7, and SCS-8) serpentine solids and the precipitated $Mg(OH)_2$ (ACS-3)

	SCS-1	SCS-4	SCS-5	SCS-6	SCS-7	SCS-8	ACS-3
LOI	14.4	4.00	14.9	17.6	16.3	17.0	23.4
Al_2O_3	0.35	0.36	0.38	0.32	0.37	0.26	0.08
BaO	<0.02	<0.02	<0.02	<0.02	<0.02	<0.02	<0.02
CaO	0.15	0.16	0.03	0.03	0.05	0.09	0.07
Fe_2O_3	4.86	5.09	1.82	0.59	2.11	4.31	0.17
K_2O	<0.02	<0.02	<0.02	<0.02	<0.02	0.03	<0.02
MgO	38.7	43.0	30.9	12.2	29.2	42.0	34.9
MnO	0.10	0.11	0.03	0.01	0.04	0.09	0.07
Na_2O	<0.02	<0.02	<0.02	<0.02	<0.02	<0.02	20.8
P_2O_5	<0.05	<0.05	<0.05	<0.05	4.41	0.03	0.03
SiO_2	39.5	41.9	48.6	69.6	47.4	37.5	0.13
SrO	<0.02	<0.02	<0.02	<0.02	<0.02	<0.02	<0.02
TiO_2	<0.02	<0.02	<0.02	<0.02	<0.02	<0.02	<0.02

Results are given as metal oxides on a weight percent basis.

volatile components (14.4%). The volatile components, given as LOI, are assumed to be mainly water that was driven off upon heating to 750 °C. The physical treatment of serpentine with high temperature steam (SCS-4) showed an increase in the amount of each major metal oxide within the sample. Because the physical treatment was intended to only remove the mineral's inherent moisture, this result was expected. Compared to the untreated parent serpentine (SCS-1), the steam activated sample's (SCS-4) lower LOI value reflects the effectiveness of the treatment, agreeing with the TGA results (Fig. 1). All but one of the chemical treatments resulted in a net loss of MgO from the serpentine. Only the NaOH activated serpentine (SCS-8) exhibited an increase in the amount of MgO. The various acids used to treat the mineral affected nearly every species within the serpentine except for SiO_2.

ICP-AES results from the acid treated solids indicated the possibility of extracting the magnesium into solution as Mg^{2+} ions. In particular, over two-thirds of the magnesium was removed during treatment with H_2SO_4 (SCS-6, Table 5). Consequently, three additional chemical treatments were performed to produce solutions with high Mg^{2+} ion concentrations. One of these treatments used H_2SO_4 to produce the precursor solution utilized for $Mg(OH)_2$ formation. $Mg(OH)_2$ was precipitated from the magnesium-rich solution produced during chemical treatment with H_2SO_4. The resulting $Mg(OH)_2$ solid (ACS-3) was found to be approximately 35% MgO by weight. The ICP-AES results shown in Table 5 also indicate that an additional 21% of the sample was Na_2O by weight, which can be attributed to the formation of sodium sulfate (Na_2SO_4) during precipitation with NaOH. The remainder of the sample's weight consisted primarily of moisture (23.4% LOI). The remaining two solutions were produced with H_2SO_4 (ACS-1) and CH_3COOH (ACS-2). ICP-AES analyses were conducted on these solutions, and the results are shown in Table 6 for the solutions as produced, as well as after neutralization with NaOH. Much of the iron, the second most dominant constituent in both solutions, was also precipitated and filtered from the solutions during the neutralization process. As the ICP-AES results in Table 6 indicate, both H_2SO_4 and CH_3COOH were effective in creating a solution with

Table 6
ICP-AES results from the analysis of solutions (ACS-1 and ACS-2) prepared by the chemical treatment of serpentine, before and after neutralization with NaOH

	ACS-1[a]	ACS-1	ACS-2[a]	ACS-2
Al	62	0.65	1	0
Ba	0	0	1	1
Ca	102	175	125	56
Fe	3000	9	1350	39
K	3	2.3	2.8	6
Mg	13,000	11,400	5250	2480
Mn	70	23	64	13
Na	7	34,800	0.1	26,660
Si	108	3.1	175	31
Sr	0	1.7	0.4	0

Results are given in parts per million by volume.
[a] Prior to neutralization with NaOH.

Mg^{2+} ions being the dominant species, although treatment with H_2SO_4 resulted in a much higher concentration.

Figs. 3–6 show the XRD patterns obtained from the analysis of the untreated parent sample (SCS-1), the high temperature steam activated sample (SCS-4), the HCl activated sample (SCS-5), and the precipitated $Mg(OH)_2$ (ACS-3), respectively. As indicated by the XRD pattern shown in Fig. 3, antigorite is the primary phase present in the untreated parent sample (SCS-1), with forsterite present in smaller amounts. Fig. 4 shows the XRD pattern obtained for the serpentine after it was activated with steam (SCS-4). The serpentine, which is essentially a hydrated form of olivine, was mostly transformed into a form of olivine known as forsterite, although antigorite is still present in the steam activated sample. The XRD pattern of the HCl activated serpentine (SCS-5) is shown in Fig. 5. Similar XRD patterns were also found for the other chemical activated samples (SCS-5, SCS-6, SCS-7, and SCS-8). In all cases, antigorite remained the primary phase present within the serpentine samples after chemical treatment. The H_2SO_4 activated sample (SCS-6) also exhibited a slightly amorphous structure. Fig. 6 shows the XRD pattern from the analysis of the precipitated $Mg(OH)_2$ (ACS-3). The pattern reveals that the sample is comprised of both brucite ($Mg(OH)_2$) and sodium sulfate (Na_2SO_4). This result, in addition to the ICP-AES results, confirms that a significant amount of Na_2SO_4 was created during the precipitation of $Mg(OH)_2$ with NaOH. This can be attributed to an excess of sodium (Na^+) and sulfate (SO_4^{2-}) ions present in the solution during the reaction.

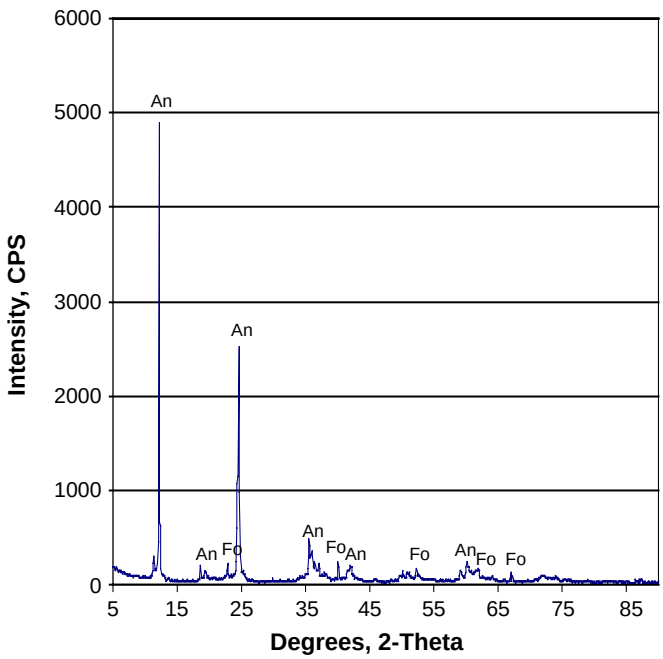

Fig. 3. The XRD pattern obtained from the analysis of the untreated parent sample (SCS-1). Peaks are identified as antigorite (An) and forsterite (Fo).

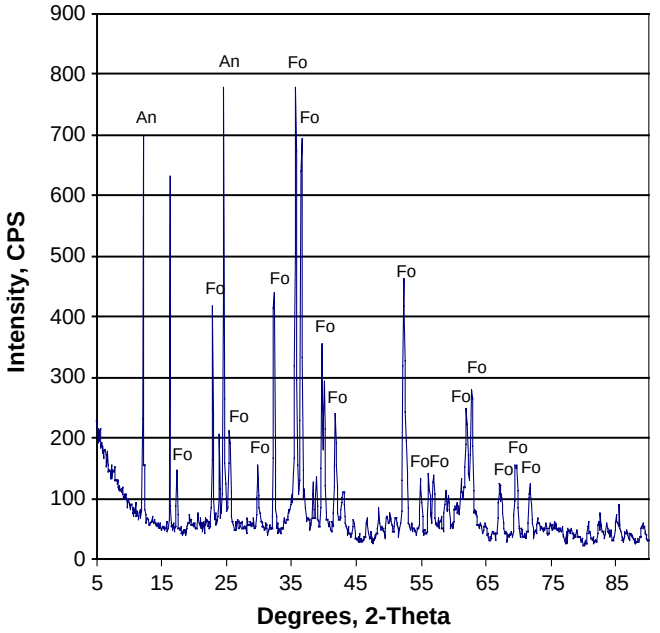

Fig. 4. The XRD pattern obtained from the analysis of the high temperature steam activated serpentine (SCS-4). Peaks are identified as forsterite (Fo) and antigorite (An).

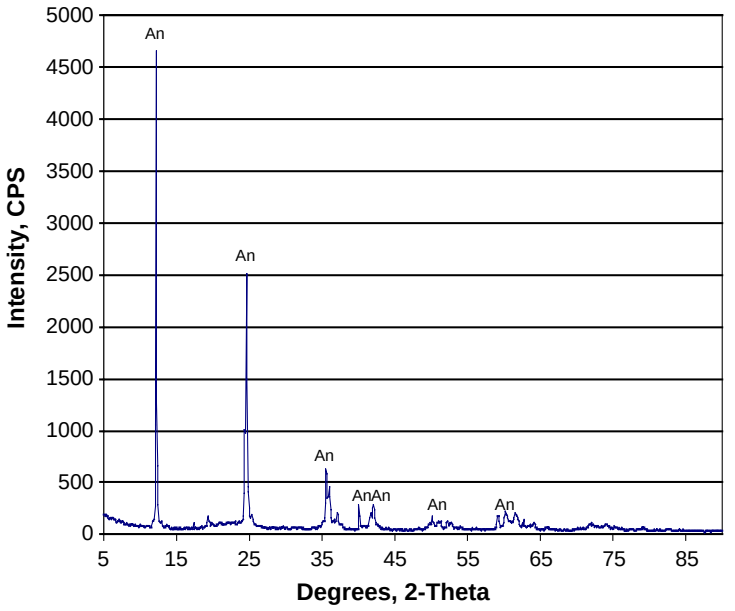

Fig. 5. The XRD pattern obtained from the analysis of the HCl activated serpentine (SCS-5). Peaks are identified as antigorite (An).

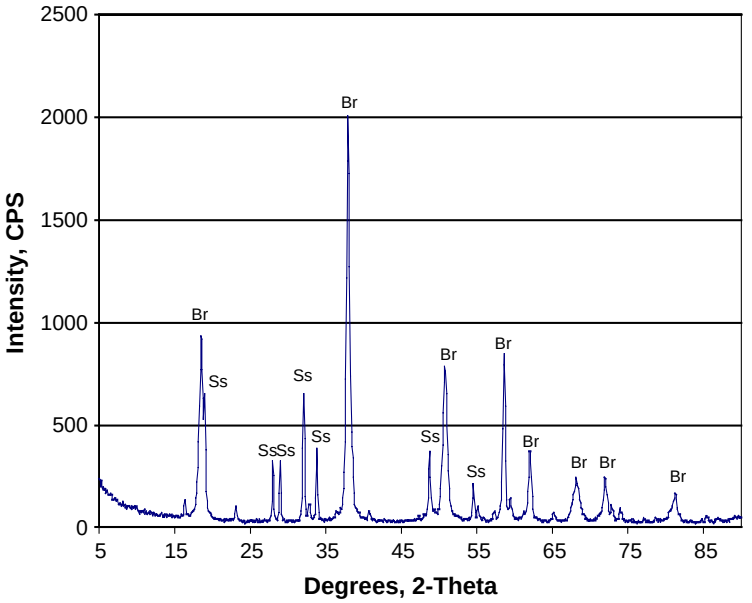

Fig. 6. The XRD pattern obtained from the analysis of the precipitated $Mg(OH)_2$ (ACS-3). Peaks are identified as brucite (Br) and sodium sulfate (Ss).

To examine the differences in the surface texture and physical appearance between the parent and activated serpentine samples, SEM analyses were performed (Figs. 7–10). As Fig. 7 illustrates, the parent Cedar Hills serpentine sample has a wide distribution of particle sizes. The particles are compact with little accessibility for CO_2 diffusion through the outer surface. The appearance of the steam activated sample (SCS-4), as shown in Fig. 8, looks somewhat changed compared to that of the parent serpentine (SCS-1, Fig. 7). The steam

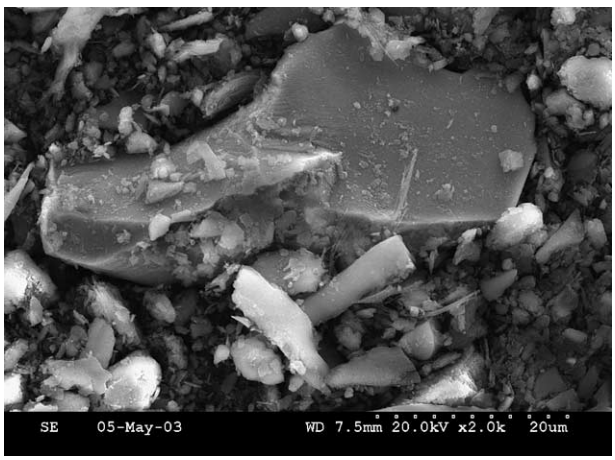

Fig. 7. The SEM image of the parent serpentine SCS-1 (2000×).

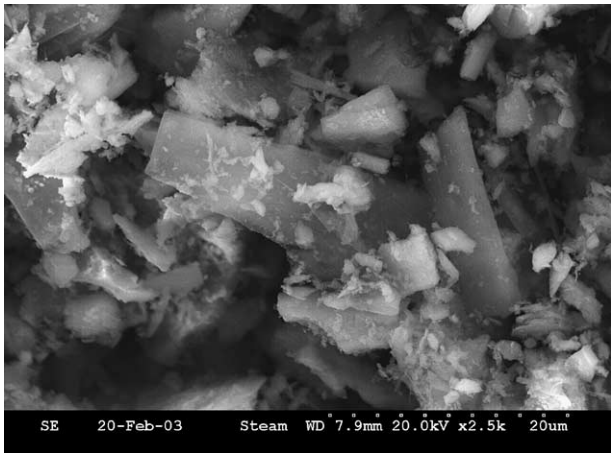

Fig. 8. The SEM image of the high temperature steam activated serpentine SCS-4 (2500×).

activation clearly has smoothen the larger particles and modified the surface. Further, the smaller particles (<2 μm) appears to be exfoliated to a certain degree that can partially account for the doubling in surface area (Table 4). Fig. 9 shows the SEM image of the H_2SO_4 activated serpentine (SCS-6). Some large particles still exist but an overall reduction in size appears to have occurred as a result of the chemical activation. This can be attributed to the dissolution of a significant portion of the mineral, including much of the MgO (Table 5). Attrition is also expected to have occurred as a result of stirring during the reaction and during the filtering process. Further, as for the steam-activated sample, the smaller particles (<5 μm) appear to be especially targeted by the activation process. Fig. 10 is an image of the H_2SO_4 activated serpentine (SCS-6) taken at a higher magnification (10,000×) and confirms the modification of the smaller particles as indicated in Fig. 9 (2000×). Fig. 10 also reveals numerous sub-micron voids in the mineral's surface of the larger particles,

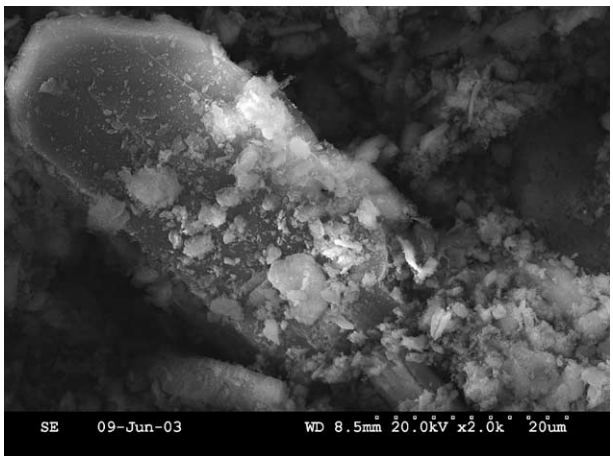

Fig. 9. The SEM image of the H_2SO_4 activated serpentine SCS-6 (2000×).

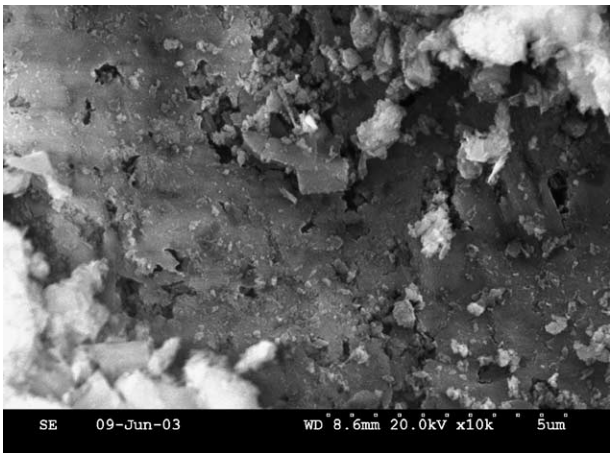

Fig. 10. The SEM image of the H_2SO_4 activated serpentine SCS-6 (10,000×).

which correspond to the areas where portions of the mineral dissolved during the chemical treatment. This is consistent with the high surface area of nearly 330 m^2/g for SCS-6.

Table 7 contains a summary of several carbonation experiments, including conversion percentages and reaction conditions. The parent sample (SCS-1) and the high temperature steam activated sample (SCS-4) were the only solid serpentine samples that underwent carbonation. The parent serpentine (SCS-1) did not react well with CO_2, reaching just 7% of the stoichiometric maximum. In contrast, the high temperature steam activated sample (SCS-4) showed a more significant conversion to $MgCO_3$, reaching nearly 60% of the stoichiometric maximum. The other physically activated serpentines (SCS-2 and SCS-3) the chemically activated serpentines (SCS-5, SCS-6, SCS-7, and

Table 7
A summary of the carbonation conversion percentages and reaction conditions of the parent and high temperature steam activated serpentines (SCS-1 and SCS-4) and the $MgSO_4$, $Mg(Ac)_2$, and $Mg(OH)_2$ solutions (ACS-1, ACS-2, and ACS-3)

Sample	Conversion percentage	Carbonation reaction conditions (temperature, pressure)
SCS-1	7.2[a]	155 °C, 126 atm
SCS-2	<0.1	155 °C, 126 atm
SCS-3	<0.1	155 °C, 126 atm
SCS-4	59.4[a]	155 °C, 126 atm
SCS-5	<0.1	155 °C, 126 atm
SCS-6	<0.1	155 °C, 126 atm
SCS-7	<0.1	155 °C, 126 atm
SCS-8	<0.1	155 °C, 126 atm
ACS-1	<0.1[b]	20 °C, 36 atm
ACS-2	<0.1[c]	20 °C, 45 atm
ACS-3	52.5[d]	20 °C, 45 atm

[a] Conversion calculated based on amount of weight gain during carbonation.
[b] Precipitate shown by XRD to contain limited amounts of carbonated magnesium minerals.
[c] Not detectable, amount of precipitate was negligible.
[d] Conversion calculated based on amount of magnesium present in the precipitate.

SCS-8) exhibited no weight gain during carbonation and thus their degree of carbonation was assumed to be negligible.

Of the three aqueous samples (ACS-1, ACS-2, and ACS-3), only the $Mg(OH)_2$ solution (ACS-3) appears to have sequestered a significant amount of CO_2. The carbonation efficiency of the $Mg(OH)_2$ solution (ACS-3) was estimated to be 52.5%. No carbonation efficiencies were calculated for the $MgSO_4$ (ACS-1) and $Mg(Ac)_2$ (ACS-2) solutions. In the case of the precipitate formed in the $MgSO_4$ solution (ACP-1), XRD analyses revealed only trace amounts of carbonated materials. Very little precipitate was recovered from the $Mg(Ac)_2$ solution, indicating that the amount of carbonation was negligible.

The results shown in Table 7 indicate that the carbonation of dissolved $Mg(OH)_2$ will occur under relatively mild conditions (20 °C and<45 atm). This is a significant improvement over previous studies that have required much more rigorous conditions (>185 °C and>125 atm). Additionally, an inherent advantage of carrying out the carbonation reaction at lower temperatures is that CO_2 solubility in water decreases with increasing temperature; the CO_2 solubility at 0 °C is 0.3346 g of gas/100 g of water, and at 60 °C the solubility decreases to 0.0576 g of gas/100 g of water [49]. Thus, the aqueous carbonation of $Mg(OH)_2$ appears to be a promising alternative to the carbonation of silicate minerals.

4. Conclusions

Physical and chemical activation of a magnesium rich mineral, a Cedar Hill serpentine, was performed to assess the products as carbonation feedstock materials for CO_2 sequestration. The physical activations were performed with air and steam, while chemical activations were performed with a suite of acids and bases. The untreated serpentine, activated serpentines, and carbonation products were characterized to determine their surface properties and assess their potential as carbonation minerals. The results indicate that the surface area of the raw serpentine, which is approximately 8 m^2/g, can be increased through physical and chemical activation methods to over 330 m^2/g. The chemical activations were more effective than the physical activations at increasing the surface area, with the 650 °C steam activated serpentine presenting a surface area of only 17 m^2/g. Sulfuric acid was the most effective acid used during the chemical activations, resulting in surface areas greater than 330 m^2/g. However, as was the case with nearly all of the chemical activations, treatment with acid resulted in the dissolution of Mg^{2+} ions from the mineral. Over 70% of the magnesium was extracted into solution during the activation with H_2SO_4. Only the NaOH activated serpentine maintained its magnesium content. Thus, although the desired increases in surface area were attained, the activated serpentines contained less MgO and had a lower potential for sequestering CO_2. Of the two acids utilized for the acid extraction studies, H_2SO_4 proved to be the most effective at removing the Mg^{2+} from serpentine. The resulting $MgSO_4$ solution was both directly forwarded to the carbonation stage and used to produce $Mg(OH)_2$. Upon titration with NaOH, $Mg(OH)_2$ was easily precipitated and removed from the $MgSO_4$ solution.

Several of the samples produced underwent varying degrees of carbonation. The steam activated serpentine underwent a 60% conversion to magnesite at 155 °C and 126 atm in

1 h, while the untreated parent sample only exhibited a 7% conversion. However, heat treatment is very energy intensive. The most promising results came from the carbonation of the $Mg(OH)_2$ solution. Based on the amount of magnesium recovered in the precipitate after the 3.5 h reaction, the carbonation efficiency was estimated to be at least 53%. Reaction products included several hydrated magnesium carbonate compounds. The carbonation reaction was conducted at ambient temperature, 20 °C, and low pressure, 45 atm. These reaction conditions are indeed a significant improvement over previous studies that required temperatures over 185 °C and pressures of at least 125 atm.

Acknowledgement

The work presented within this paper was funded by the U.S. Department of Energy through their University Coal Research Program, under grant DE-FG2601-NT41286. It was also supported by the Energy Institute and the Department of Energy and Geo-Environmental Engineering at the Pennsylvania State University. The authors would also like to thank W.K. O'Connor from U.S. DOE Albany Research Center for providing the serpentine samples and helpful discussions.

References

[1] H.J. Herzog, CO_2 Capture, Reuse, and Sequestration Technologies for Mitigating Global Climate Change, DOE/PC/96354-98, MIT Laboratory for Energy and the Environment, Cambridge, Massachusetts, 1998.
[2] H. Bearat, M.J. McKelvy, A.V.G. Chizmeshya, R. Sharma, R.W. Carpenter, Journal of the American Ceramic Society 85 (2002) 742.
[3] K.S. Lackner, D.P. Butt, C.H. Wendt, H.J. Ziock, Proceedings of Advanced Coal-Based Power and Environmental systems '98, Morgantown, West Virginia, 1998 (July 21–23), pp. PA.8.
[4] K.S. Lackner, P. Grimes, H.J. Ziock, Proceedings of the 24th Annual Technical Conference on Coal Utilization and Fuel Systems, Clearwater, Florida, March 8–11, 1999, p. 885.
[5] R.P. Walters, Z.Y. Chen, P. Goldberg, K. Lackner, M. McKelvy, H. Ziock, Mineral Carbonation: A Viable Method for CO2 Sequestration, The National Energy Technology Laboratory, Morgantown, West Virginia, 1999.
[6] K.S. Lackner, D.P. Butt, C.H. Wendt, Proceedings of the 22nd International Technical Conference on Coal Utilization and Fuel Systems, Clearwater, Florida, March 16–19, 1997.
[7] IPCC, Climate change 2001: the scientific basis, in: J.T. Houghton, Y. Ding, D.J. Griggs, M. Noguer, P.J. van der Linden, X. Dai, D. Maskell, C.A. Johnson (Eds.), Contribution of Working Group I to the Third Assessment Report of the Intergovernmental Panel on Climate Change, Cambridge University Press, New York, 2001.
[8] IPCC, Climate change 1996: the science of climate change, in: J.T. Houghton, L.G.M. Filho, B.A. Callander, N. Harris, A. Kattenberg, K. Maskell (Eds.), Contribution of Working Group I to the Second Assessment Report of the Intergovernmental Panel on Climate Change, Cambridge University Press, New York, 1996.
[9] Energy Information Administration, Emissions of Greenhouse Gases in the United States 2001, DOE/EIA-0573, Energy Information Administration, Office of Integrated Analysis and Forecasting, U.S. Department of Energy, Washington, DC, 2002.
[10] C.D. Keeling, T.P. Whorf, Atmospheric CO_2 records from sites in the SIO air sampling network, Trends: A compendium of data on global change, U.S. Department of Energy, Carbon Dioxide Information Analysis Center, Oak Ridge National Laboratory, Oak Ridge, Tennessee, 2003.
[11] K.S. Lackner, D.P. Butt, C.H. Wendt, Proceedings of the 23rd International Conference on Coal Utilization and Fuel Systems, Clearwater, Florida, March 9–13, 1998.

[12] DOE report DOE/SC/FE-1 "Carbon Sequestration: Research and Development." in: D. Reichle, B. Kane, J. Houghton and J. Elkmann (Eds.), Office of Science, Office of Fossil Energy, U.S. Department of Energy, Washington, DC (1999).
[13] D.J. Fauth, J.P. Baltrus, Y. Soong, J.P. Knoer, B.H. Howard, W.J. Graham, M.M. Maroto-Valer, J.M. Andrésen, in: M.M. Maroto-Valer, C. Song, Y. Soong (Eds.), Environmental Challenges and Greenhouse Gas Control for Fossil Fuel Utilization in the 21st Century, Kluwer Academic/Plenum Publishers, New York, 2002, pp. 107–117.
[14] D.J. Fauth, J.P. Baltrus, Y. Soong, J.P. Knoer, B.H. Howard, W.J. Graham, M.M. Maroto-Valer, J.M. Andrésen, Preprints-American Chemical Society. Division of Fuel Chemistry 46 (1) (2001) 278.
[15] K.S. Lackner, Proceedings of the Advanced Process Concepts for Carbon Management Workshop, Dallas, Texas, March 20–21, 2000.
[16] D.P. Butt, K.S. Lackner, C.H. Wendt, Y.S. Park, A. Benjamin, D.M. Harradine, T. Holesinger, M. Rising, K. Nomura, World Resource Review 9 (3) (1997) 324.
[17] F. Goff, G.D. Guthrie, B. Lipin, M. Fite, S.J. Chipera, D. Counce, E. Kluk, H.J. Ziock, Evaluation of Ultramafic Deposits in the Eastern United States and Puerto Rico as Sources of Magnesium for Carbon Dioxide Sequestration, Los Alamos National Laboratory, Los Alamos, New Mexico, 2000, LA-13694-MS.
[18] F. Goff, G.D. Guthrie, D. Counce, E. Kluk, D. Bergfeld, M. Snow, Preliminary Investigations on the Carbon Dioxide Sequestering Potential of Ultramafic Rocks, Los Alamos National Laboratory, 1997, LA-13328-MS.
[19] D.C. Dahlin, W.K. O'Connor, D.N. Nilsen, G.E. Rush, R.P. Walters, P.C. Turner, Proceedings of the 17th Annual International Pittsburgh Coal Conference, Pittsburgh, Pennsylvania, September 11–15, 2000, pp. 18–23.
[20] P. Goldberg, Z.Y. Chen, W. O'Connor, R. Walters, H. Ziock, Journal of Energy and Environmental Research 1 (1) (2001) 117.
[21] W. Seifritz, Nature 345 (7) (1990) 486.
[22] H.J. Herzog, Carbon Sequestration via Mineral Carbonation: Overview and Assessment, MIT Laboratory for Energy and the Environment, Cambridge, Massachusetts, 2002.
[23] W.K. O'Connor, D.C. Dahlin, D.N. Nilsen, G.E. Rush, R.P. Walters, P.C. Turner, Proceedings of the 1st National Conference on Carbon Sequestration, Washington, DC, May 14–17, 2001, p. 6C2.
[24] W.K. O'Connor, D.C. Dahlin, G.E. Rush, C.L. Dahlin, W.K. Collins, Minerals and Metallurgical Processing 19 (2) (2002) 95.
[25] R. Zevenhoven, J. Kohlmann, A.B. Mukherjee, Proceedings of the 27th international technical conference on coal utilization and fuel systems, Clearwater, Florida, March 4–7, 2002.
[26] J. Winters, Mechanical Engineering 125 (2) (2003) 46.
[27] W.K. O'Connor, D.C. Dahlin, P.C. Turner, R. Walters, Proceedings of the 2nd Dixy Lee Ray Memorial Symposium: Utilization of Fossil Fuel-Generated Carbon Dioxide in Agriculture and Industry, Washington, DC, August 31–September 2, 1999.
[28] K.S. Lackner, C.H. Wendt, D.P. Butt, E.L. Joyce, D.H. Sharp, Energy 20 (11) (1995) 1153.
[29] P. Goldberg, R. Walters, Proceedings of the 6th International Conference on Greenhouse Gas Control Technologies, Kyoto, Japan, October 1–4, 2002.
[30] P. Petrovski, M. Gligorio, M. Nisevic, M. Begagic, in: P. Vincenzini (Ed.), High Tech Ceramics, Elsevier Science Publishers, Amsterdam, 1987.
[31] Q. Zhang, K. Sugiyama, F. Saito, Hydrometallurgy 45 (1997) 323.
[32] K. Kosuge, K. Shimada, A. Tsunashima, Chemical Materials 7 (12) (1995) 2241.
[33] B.S. Girgis, W.E. Mourad, Journal of Applied Chemistry & Biotechnology 26 (9) (1976) 9.
[34] J.E. Dutrizac, T.T. Chen, C.W. White, in: H.I. Kaplan, J. Hryn, B. Clow (Eds.), Proceedings of Magnesium Technology 2000, Nashville, Tennessee, March 12–16, 2000, p. 41.
[35] K.S. Lackner, D.P. Butt, C.H. Wendt, D.H. Sharp, Proceedings of the 21st international conference on coal utilization and fuel systems, Clearwater, Florida, March 18–21, 1996.
[36] C.H. Wendt, D.P. Butt, K.S. Lackner, H.J. Ziock, Thermodynamic Calculations for Acid Decomposition of Serpentine and Olivine in MgCl2 Melts—Report II, Los Alamos National Laboratory, Los Alamos, New Mexico, 1998, LA-UR-98-4529.
[37] A.H.A. Park, R. Jadhav, L.S. Fan, Canadian Journal of Chemical Engineering 81 (2003) 885.

[38] W.K. O'Connor, D.C. Dahlin, G.E. Rush, S.J. Gerdemann, L.R. Penner, Energy and economic considerations for ex situ aqueous mineral carbonation, Proc., 29th International Technical Conference on Coal Utilization and Fuel Systems, Coal Technology Association, Clearwater, FL, 2004.
[39] S.J. Gerdemann, D.C. Dahlin, W.K. O'Connor, L.R. Penner, Proceedings of the 6th International Conference on Greenhouse Gas Control Technologies, Kyoto, Japan, October 1–4, 2002.
[40] M.M. Maroto-Valer, D.J. Fauth, M.E. Kuchta, Y. Zhang, J.M. Andrésen, Y. Soong, Proceedings of the 18th Annual International Pittsburgh Coal Conference, Pittsburgh, Pennsylvania, September 23-01, 2001.
[41] H.J. Herzog, Carbon Sequestration via Mineral Carbonation: Overview and Assessment, Massachusetts Institute of Technology Laboratory for Energy and the Environment, 2002, 11 pp.
[42] IEA, CO_2 Storage as Carbonate Minerals. Study Prepared by CSMA Minerals Lmtd. Commissioned by International Energy Association, Greenhouse R&D Programme (1999) 124 pp.
[43] D.N. Nilsen, G. Hundley, Preliminary Feasibility Study of the Sequestration of Carbon dioxide Gas with Minerals: a Study of the LANL Aqueous Process. Albany Research Center, US DOE, DOE/ARC-TR-99-003, 1999.
[44] V.E. Barnes, D.A. Shock, W.A. Cunningham, Utilization of Texas Serpentine, The University of Texas, Bureau of Economic Geology, No. 5020, 1950.
[45] Hellmuth R. Brandeburg, Process for Recovering Magnesium Oxide. U.S. Patent 2,210,892 (1940).
[46] Samuel Peacock, Process for Producing Magnesium Compounds. U.S. Patent 1,205,659 (1916).
[47] Louis L. Jackson, Process for Extracting Metals From Silicates. U.S. Patent 1,305,969 (1919).
[48] Walter H. MacIntire, Process for Producing Anhydrous Magnesium Sulphate. U.S. Patent 2,298,493 (1942).
[49] R. Crovetto, R.H. Wood, Fluid Phase Equilibria 74 (2002) 271.